AN ABSTRACT OF THE THESIS OF

SUNG SOO KIM (Name) for the MASTER OF SCIENCE (Degree)

in Mechanical Engineering (Major) presented on Dec. 14, 1970 (Date)

Title: AN EXPERIMENTAL STUDY OF NATURAL CONVECTION IN AIR BETWEEN A VERTICAL ISOTHERMAL FLAT PLATE AND A PARALLEL INSULATED FLAT PLATE

Redacted for privacy

Abstract approved: _____
Dr. James R. Welty

Natural convection heat transfer in air between two vertical plates 38 by 24 inches was investigated in this work with spacings between the plates of 0.625, 1.0 and 1.75 inches. One plate was isothermal and the other adiabatic.

To measure the point velocities in the air layer a very thin quartz fiber 0.0005 in. in diameter was used. An iron-constantan thermocouple 0.001 in. in diameter was used for local temperature measurement. Velocity and temperature profiles were obtained at several positions along the plate for each spacing between the plates.

An equation in the form

$$Nu_x = 0.348\,(Gr_x(x/W))^{0.241}$$

best describes the local heat transfer characteristics for this study.

An Experimental Study of Natural Convection in Air Between a Vertical Isothermal Flat Plate And a Parallel Insulated Flat Plate

by

Sung Soo Kim

A THESIS

submitted to

Oregon State University

in partial fulfillment of
the requirements for the
degree of

Master of Science

June 1971

APPROVED:

Redacted for privacy

Professor of Mechanical Engineering
in charge of major

Redacted for privacy

Head of Department of Mechanical Engineering

Redacted for privacy

Dean of Graduate School

Date thesis is presented December 14, 1970

Typed by Muriel Davis for Sung Soo Kim

ACKNOWLEDGMENT

In presenting this work, I wish to express my sincerest gratitude to Dr. James R. Welty for his careful guidance and understanding throughout this work and the writing of this manuscript.

Deep appreciation is also expressed to Mr. David E. Stock and other graduate fellows in our department for their invaluable suggestions and friendship during the experiment.

Special thanks is given to my wife, Duk Hee, for her companionship and encouragement. Her great assistance with the experiment and the typing of this manuscript is also appreciated.

TABLE OF CONTENTS

LIST OF FIGURES

LIST OF TABLES

NOMENCLATURE

A	heat transfer area
c_p	specific heat under constant pressure
g	gravitational acceleration
h	convective heat transfer coefficient
H	total height of vertical plate
k	conductivity of fluid
L	width of plate
p	pressure
q	heat transferred
T	temperature
U	velocity component in x-direction
V	velocity component in y-direction
W	distance between plates
x	direction parallel to the heated plate
y	direction normal to the heated plate

Parameters

Gr_x	local Grashof number $\dfrac{\beta g x^3 (T_s - T_\infty)}{\nu^2}$
Nu_x	local Nusselt number hx/k
Pr	Prandtl number $\mu c_p/k$

Greek symbols

α	thermal diffusivity
β	coefficient of volumetric expansion
δ	deflection of quartz fiber
θ	dimensionless temperature
μ	absolute viscosity
ψ	stream function
ρ	density
η	similarity parameter
σ	dimensionless pressure
ϕ	dimensionless density
ν	kinematic viscosity

Subscripts

H	overall mean average over the hot plate
m	mean value
r	reference conditions
s	hot surface
x	local point
∞	ambient conditions

Superscripts

$'$	first derivative
$''$	second derivative
$'''$	third derivative

AN EXPERIMENTAL STUDY OF NATURAL CONVECTION IN AIR BETWEEN A VERTICAL ISOTHERMAL FLAT PLATE AND A PARALLEL INSULATED FLAT PLATE

INTRODUCTION

Two important types of flow problems involving heat transfer are those of forced and free convection. By forced-convection flow is meant flows maintained mechanically as, for example, by a pressure drop or an agitator. Free convection flow, on the other hand, results from the action of body forces on the fluid, that is, forces which are proportional to the mass or the density of the fluid.

Experimental investigation in this study considered the special case of free-convection flow between two vertical plates one being an isothermal hot plate and the other an adiabatic plate.

The equations expressing conservation of mass, momentum and energy for laminar free convection in a boundary layer when the system is assumed to be a Newtonian, two-dimensional, steady, laminar, incompressible and constant property flow, are

$$\frac{\partial U}{\partial x} + \frac{\partial V}{\partial y} = 0 \tag{1}$$

$$U\frac{\partial U}{\partial x} + V\frac{\partial U}{\partial y} = g\beta(T-T_\infty) + \nu\frac{\partial^2 U}{\partial y^2} \tag{2}$$

$$U\frac{\partial T}{\partial x} + V\frac{\partial T}{\partial y} = \alpha\frac{\partial^2 T}{\partial y^2} \tag{3}$$

When the temperature differences involved are relatively small as in the present investigation, a simplified treatment assuming all fluid properties constant and neglecting heat transfer via radiation does not appear unreasonable.

Due to the complexity of the governing equations above, analytical solutions are known to exist only in a limited number of simple cases as laminar free convection from a vertical plate with either uniform temperature or heat flux. As a result much effort has been made to obtain satisfying experimental equations from experimental data.

Throughout this work, reference will be made to distances along and/or normal to the heated plate and the velocity components in these directions. In order to avoid confusion in this matter, the point $x = 0$, $y = 0$ refers to the bottom of the heated plate. The positive x-axis is parallel to the heated plate and the positive y-axis is defined to be normal to the heated plate.

Consider the vertical layer shown in Figure 1 with dimensions L, W and H. By means of dimensional analysis, it can be shown that the heat transferred across such layers is a function of the local Grashof number, the Prandtl number, the fluid layer-to-height ratio and width-to-height ratio. The dimensionless heat transfer coefficient, the local Nusselt number, can be written as a function of these quantities:

A Container with acetone vapor

B Hot acetone vapor

C Boiling liquid acetone

D Adiabatic wall

E Hot aluminum plate

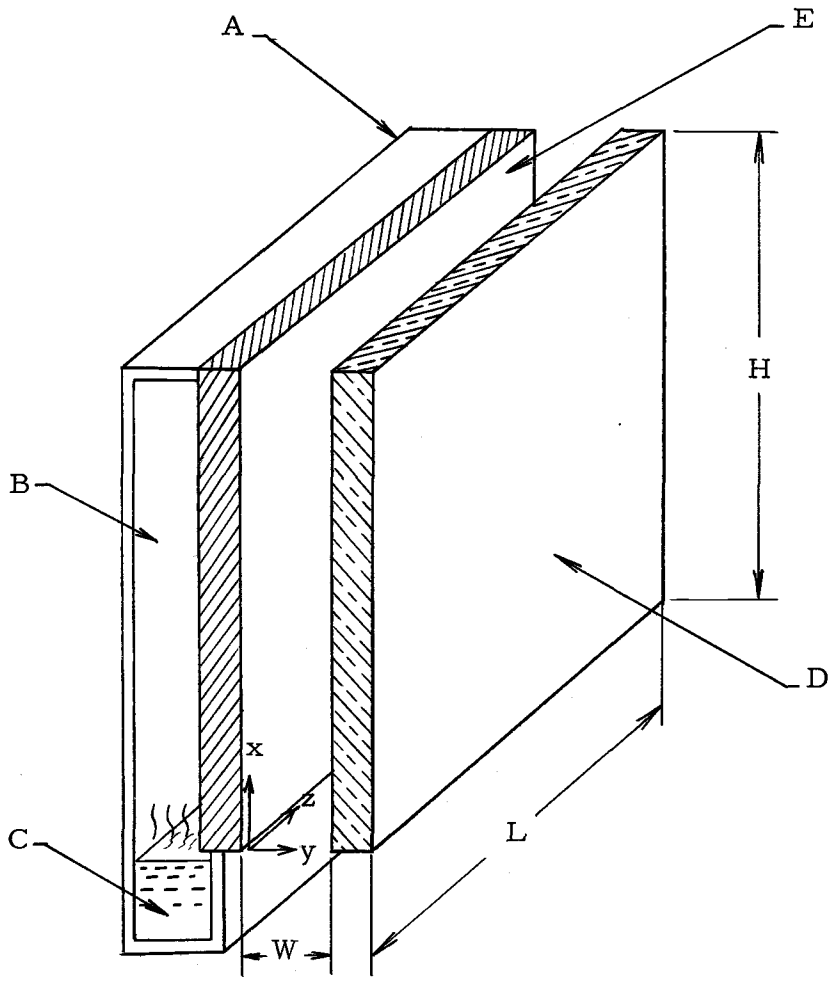

Figure 1. Overall dimensions and description of the vertical plates.

$$Nu_x = f(Gr_x, Pr, x/W, H/W)$$

$$= aGr_x^{b}Pr^{c}(x/W)^{d}(H/W)^{e}$$

where

Nu_x = hx/k, the local Nusselt number

$Gr_x = \frac{\beta g(T_s - T_m)x^3}{\nu^2}$, the local Grashof number

H = height of vertical plane walls

L = width of vertical plane walls

W = width of air layer

$Pr = \mu c_p/k$, Prandtl number

a, b, c, d, e, = constants

For moderate temperature differences between the hot plate and air layer, flow is a function of two factors, local Grashof number, Gr_x, and/or spacing distance between the two plates. Usually the criterion of turbulence for natural convection flow along a single vertical heated plate is the local Grashof number only. In air laminar flow occurs when the local Grashof number is less than 10^8 and turbulent flow occurs for Gr_x greater than 10^{10}. When the spacing is larger than the boundary layer thickness, the decisive factor determining turbulence is the Grashof number as in the single vertical heated plate case. But when the spacing is smaller than the boundary layer

thickness, it will be influenced not only by the Grashof number but also by the spacing distance.

LITERATURE REVIEW

Of prime concern in this literature review were articles published from 1950 to the present, but it is meaningful to survey some important developments in the field before this period.

The first analytical solution concerning heat transfer between a single isothermal vertical wall and the ambient was accomplished by L. Lorenz (5) in 1881. He made several simplifying assumptions including the following:

1. The horizontal component, V, of the air velocity was neglected.

2. The vertical velocity, U, remained constant at any vertical plane parallel to the wall so that $\frac{\partial U}{\partial x} = 0$.

3. At the upper edge of the vertical wall where $x = H$ in. the vertical velocity, U, and the temperature were both considered constant.

By solving the equations expressing conservation of momentum and energy with these assumptions he obtained the convective heat transfer coefficient for the entire surface.

$$h = N \sqrt[4]{\frac{g c_p \rho_\infty^2 k^3 (T_s - T_\infty)}{\mu H T_\infty}} \qquad (4)$$

where N is a numerical constant which is 0.548 for air at

atmospheric pressure. The average rate of heat transfer by convection from the vertical surface to the surroundings is

$$q/A = h(T_s - T_\infty) \text{Btu/ft}^2\text{hr}$$

or

$$q/A = 0.548\sqrt[4]{\frac{g c_p \rho_\infty^2 k^3}{\mu H T_\infty}} (T_s - T_\infty)^{5/4} \qquad (5)$$

This shows the average rate of heat transfer to be proportional to the 5/4 power of the temperature difference between the wall and the surroundings. This particular result has been shown to be correct by both experimental and analytical results since Lorenz' time. Although, due to the several too simple assumptions, Lorenz's result was not applicable in the range of excess temperature ($\theta = T_s - T_\infty$) from 0 to 20 F, the relationship between q/A and θ is worth mentioning in light of that indicated above.

A significant improvement was achieved by E. Schmidt and W. Beckmann (8) in 1930. They solved, with the aid of E. Pohlhausen, a modified set of the mass, momentum and energy equations by introducing the stream function and two variables which allowed the resulting equations to be calculated numerically.

Their analysis started with the basic equations involved for a steady state condition:

$$\frac{\partial U}{\partial x} + \frac{\partial V}{\partial y} = 0 \tag{6}$$

$$U\frac{\partial U}{\partial x} + V\frac{\partial U}{\partial y} = \nu\left(\frac{\partial^2 U}{\partial x^2} + \frac{\partial^2 U}{\partial y^2}\right) + g\left(\frac{\rho_\infty - \rho}{\rho}\right) \tag{7}$$

$$U\frac{\partial V}{\partial x} + V\frac{\partial V}{\partial y} = \nu\left(\frac{\partial^2 V}{\partial x^2} + \frac{\partial^2 V}{\partial y^2}\right) \tag{8}$$

$$U\frac{\partial T}{\partial x} + V\frac{\partial T}{\partial y} = \alpha\left(\frac{\partial^2 T}{\partial x^2} + \frac{\partial^2 T}{\partial y^2}\right) \tag{9}$$

Schmidt and Beckmann chose to consider an incompressible flow with the buoyant effect introduced in the last term of equation (7). Considering a low pressure isobaric field, the buoyancy term, with the use of the ideal gas relationship, was approximated to be;

$$\frac{\rho_\infty - \rho}{\rho} = \frac{T - T_\infty}{T_\infty} \tag{10}$$

They used the following logic which led to the deletion of some of the terms in equations (6) through (9).

Since $V << U$ for all x except in the vicinity of the lower edge of the plate, the entire momentum equation in the y direction, equation (8), was eliminated.

Since $\partial T/\partial x < \partial T/\partial y$ which justifies $\partial^2 T/\partial x^2 << \partial^2 T/\partial y^2$, then $\partial^2 T/\partial x^2$ was eliminated.

Similarly, $\partial U/\partial x < \partial U/\partial y$, thus $\partial^2 U/\partial x^2 << \partial^2 U/\partial y^2$, so $\partial^2 U/\partial x^2$ was eliminated.

With these simplifications, the equations (6) through (9) became:

$$\frac{\partial U}{\partial x} + \frac{\partial V}{\partial y} = 0 \tag{11}$$

$$U\frac{\partial U}{\partial x} + V\frac{\partial V}{\partial y} = \nu\left(\frac{\partial^2 U}{\partial y^2}\right) + g\left(\frac{T_s - T_\infty}{T_\infty}\right)\theta \tag{12}$$

$$U\frac{\partial \theta}{\partial x} + V\frac{\partial \theta}{\partial y} = \alpha\frac{\partial^2 \theta}{\partial y^2} \tag{13}$$

where θ was defined as $\dfrac{T - T_\infty}{T_s - T_\infty}$.

Introducing the stream function

$$U = \frac{\partial \psi}{\partial y} \qquad \text{and} \qquad V = -\frac{\partial \psi}{\partial x}$$

equations (11) through (13) became:

$$\frac{\partial \psi}{\partial y}\frac{\partial^2 \psi}{\partial x \partial y} - \frac{\partial \psi}{\partial x}\frac{\partial^2 \psi}{\partial y^2} = \nu\frac{\partial^3 \psi}{\partial y^3} + g\left(\frac{T_s - T_\infty}{T_\infty}\right)\theta \tag{14}$$

$$\frac{\partial \psi}{\partial y}\frac{\partial \theta}{\partial x} - \frac{\partial \psi}{\partial x}\frac{\partial \theta}{\partial y} = \alpha\frac{\partial^2 \theta}{\partial y^2} \tag{15}$$

Using a similarity parameter defined by Pohlhausen

$$\eta = C\frac{y}{x^{1/4}} \tag{16}$$

where

$$C = \left[\frac{(T_s - T_\infty)g}{4\nu^2 T_\infty}\right]^{1/4}$$

the functions ψ and θ were transformed to $F(\eta)$ and $G(\eta)$ as

$$\psi(x, y) = 4\nu C x^{3/4} F(\eta) \tag{17}$$

$$\theta(x, y) = G(\eta) \tag{18}$$

Then the velocity components became:

$$U = 4\nu x^{1/2} C F'(\eta)$$

$$V = \nu C x^{-1/4} (\eta F'(\eta) - 3F(\eta))$$

and the governing equations became:

$$F''' + 3FF'' - 2(F')^2 + G = 0 \tag{19}$$

$$G'' + 3PrFG' = 0 \tag{20}$$

where the primed values are successive derivatives with respect to η.

The transformed boundary contions were

$$F = F' = 0 \qquad G = 1 \qquad \text{at } \eta = 0$$

$$F' = 0 \qquad G = 0 \qquad \text{at } \eta = \infty$$

for air with $Pr = 0.733$

$$q/A = h_x(T_s - T_\infty) = -k \frac{\partial T}{\partial y})_{y=0}$$

$$= -k (T_s - T_\infty) C x^{-1/4} \frac{\partial \theta}{\partial \eta})_{\eta=0} \tag{21}$$

$$Nu_x = \frac{h_x x}{k} = -\frac{\partial \theta}{\partial \eta})_{\eta=0} \left(\frac{Gr_x}{4}\right)^{1/4} \tag{22}$$

where for air $\frac{\partial \theta}{\partial \eta})_{\eta=0} = 0.508$

To get the mean Nusselt number for a plate of height, H,

$$h_H = \frac{1}{H}\int_0^H h_x dx \qquad (23)$$

$$= 0.508\,\frac{k}{H}\int_0^H \left(\frac{g(T_s - T_\infty)}{4\nu^2 T}\right)^{1/4} x^{-1/4} dx$$

$$= 0.677\,\frac{k}{H}\left(\frac{Gr_H}{H}\right)^{1/4}$$

So,

$$Nu_H = \frac{h_H H}{k} = 0.677\left(\frac{Gr_H}{4}\right)^{1/4} = 0.478\,(Gr_H)^{1/4} \qquad (24)$$

Further analytical results on this problem were achieved by S. Ostrach (6) in 1953. He started with the complete set of mass, momentum and energy equations expressed in Cartesian tensor notation. To make the equations more realistic, an assumption was made about density, viscosity and thermal conductivity coefficients as,

$$d\rho = \rho(k\,dP - \beta\,dT)$$

$$\mu = \mu_\infty\left(\frac{T}{T_\infty}\right)^m$$

$$k = k_\infty\left(\frac{T}{T_\infty}\right)^n$$

He converted all terms of the basic equations by introducing the stream function and then made the following transformations to retain the dominant part expressed in Grashof number to the highest power for each individual term.

$$y = Gr^{r}\,\overline{y}\,, \qquad \psi = Gr^{s}\,\overline{\psi}\,, \qquad \sigma = Gr^{t}\,\overline{\sigma}$$

$$\phi = \overline{\phi} \qquad \text{and} \qquad \theta = \overline{\theta}$$

By proper choice of r, s and t, he showed a transformation of the type given provided a means for making the important terms in the differential equations the same order in Gr. With final simplification by means of a similarity transformation, he obtained the same ordinary differential equations as those found by Schmidt and Beckmann before. Although the final equations obtained by his method were the same as those of Schmidt and Beckmann, this more general approach not only clearly demonstrated the significance of all the important parameters and assumptions, hence a better understanding of this type of flow but also indicated the quantitative limitations of the theory.

An exact solution of the laminar boundary layer equations for free convection from a vertical plate having uniform surface heat flux has been obtained by E.M. Sparrow and J.L. Gregg (9). Heat transfer results obtained from the von Karman-Pohlhausen method also are shown to be in good agreement with those from the exact solution. They started from the usual equations of conservation of mass, momentum and energy as equations (11) through (13) with the boundary conditions

$$U = V = 0 \qquad -k\left(\frac{\partial T}{\partial y}\right)_{y=0} = q(\text{constant}) \qquad \text{at } y = 0$$

$$U = 0 \qquad T = T_{\infty} \qquad \text{at } y = \infty$$

Transforming the basic equation by changing the (x, y) coordinate system to the (x, η) system with the following substitutions:

$$\eta = C_1 \frac{y}{x^{1/5}}$$

$$F(\eta) = \frac{\psi}{C_2 x^{4/5}}$$

$$\theta(\eta) = \frac{C_1 (T_\infty - T)}{\frac{x^{1/5} q}{k}}$$

where

$$C_1 = \left(\frac{g\beta q}{5k\nu^2}\right)^{1/5}, \qquad C_2 = \left(\frac{5^4 g\beta\nu^3}{k}\right)^{1/5}$$

they finally obtained differential equations as:

$$F''' - 3(F')^2 + 4FF'' - \theta = 0 \tag{25}$$

$$\theta'' + Pr(4\theta' F - \theta F') = 0 \tag{26}$$

with the boundary conditions

$F = 0 \qquad F' = 0 \qquad \theta' = 0 \qquad$ at $\eta = 0$

$F' = 0 \qquad \theta = 0 \qquad$ at $\eta = \infty$

From this system the surface temperature variation, local Nusselt number, velocity and temperature distributions were obtained as follows:

$$T_s - T_\infty = -5^{1/5}\theta(0)\,\frac{qx}{k}\left(\frac{g\beta qx^4}{\nu^2 k}\right)^{-1/5}$$

$$= -5^{1/5}\theta(0)\,\frac{qx}{k}\,Gr_x^* \qquad (27)$$

where the modified Grashof number based on x is

$$Gr_x^* = \frac{g\beta qx^4}{\nu^2 k} = \frac{g\beta x^4 (h(T_s - T_\infty))}{\nu^2 k}$$

$$= \left(\frac{g\beta x^3 (T_s - T_\infty)}{\nu^2}\right)\left(\frac{hx}{k}\right) = Gr_x Nu_x$$

and

$$Nu_x = -\frac{Gr_x^{*\,1/5}}{5^{1/5}\theta(0)} \qquad (28)$$

$\theta(0)$ was calculated for Prandtl numbers of 0.1, 1, 10, 100.

Experimental results were compared with theory and the agreement was found to be good. Heat transfer results obtained from the von Karman-Pohlhausen method also were shown to be in good agreement with those from the exact solution. It was demonstrated that when average Nusselt numbers were calculated for a plate with uniform heat flux using the temperature difference half way along the height, the results were very close to those for a uniform temperature plate.

J. T. Bevans (1) performed an experiment in 1956 concerned with additional natural convection heat transfer of a vertical isothermal plate to detect the influence on the local Nusselt number coming

from the unheated starting length and blocking obstruction which was a horizontal flat plate placed some distance from the bottom end. He said that the effect of an unheated starting length was negligible within experimental accuracy. He correlated his experimental data with the equation

$$Nu_x = 0.41 (Gr_x Pr)^{1/4} \tag{29}$$

and observed a disturbance to occur within the boundary layer at a GrPr modulus of approximately 10^8, which is slightly lower than the critical value of 2.8×10^8 obtained by Eckert.

He observed the effect of the obstruction for which GrPr modulus was obtained by changing the ambient and plate temperature with the same blocking distance. He concluded from the latter results that for GrPr moduli less than $(GrPr)_{critical}$ the obstruction had no effect. An arbitrary limit of the effect of the obstruction was obtained by

$$(GrPr)_{crit} = (GrPr)_{blocking} \left(\frac{x_{blocking} - 2\delta_{blocking}}{x_{blocking}}\right)^3 \tag{30}$$

where the value of $\delta_{blocking}$ was the boundary layer thickness occurring at $x_{blocking}$ as given by the approximate theory of Eckert for a Prandtl number of 0.7.

An analysis was made of the variable fluid property problem for laminar free convection on an isothermal vertical plate by E. M. Sparrow and J. L. Gregg (10) in 1957. For a number of specific

cases, solutions of the boundary layer equations appropriate to the variable-property situation were carried out for gases and liquid mercury. Utilizing these findings they presented a simple and accurate shorthand procedure for calculating free convection heat transfer under variable-property conditions. It involved the use of results which had been obtained for constant property fluids, and a set of rules (called reference temperatures) for extending these constant-property results to variable-property situations. For gases, the constant-property heat transfer results were generalized to the variable property situation by replacing β (thermal expansion coefficient) by $1/T_\infty$ and evaluating the other properties at $T_r = T_s - 0.38\,(T_s - T_\infty)$. The error in the heat transfer predicted from the constant-property results by using this reference temperature was at most 0.6% over the entire range $1/4 \leq T_s/T_\infty \leq 4$. They also stated that the use of T_f (film temperature) as a reference temperature provided heat transfer results which would be adequate for almost all engineering purposes.

An integral solution for natural convection adjacent to a heated vertical surface may also be achieved. The resulting equations are:

$$\frac{\partial}{\partial x}\int_0^\delta u^2\,dy = g\beta\int_0^\delta (T - T_\infty)\,dy - \nu\left(\frac{\partial u}{\partial y}\right)_{y=0} \qquad (31)$$

$$\frac{\partial}{\partial x}\int_0^{\delta} u(T - T_\infty)dy = -\alpha\frac{\partial T}{\partial y})_{y=0} \qquad (32)$$

Assuming the thermal and velocity boundary layer thicknesses to be equal and further assuming velocity and temperature profiles of reasonable form the following results have been obtained.

In laminar flow for constant wall temperature

$$Nu_x = 0.505\ Pr^{1/2}(0.952 + Pr)^{-1/4}Gr_x^{1/4} \qquad (33)$$

and for constant heat flux

$$Nu_x = 0.547\ Pr^{1/2}(0.8 + Pr)^{-1/4}Gr_x^{1/4} \qquad (34)$$

In turbulent flow for constant wall temperature

$$Nu_x = 0.0295\ Pr^{7/15}(1 + 0.494(Pr)^{2/3})^{-2/5}(Gr_x)^{2/5} \qquad (35)$$

for constant heat flux

$$Nu_x = 0.0297\ Pr^{7/15}(1 + 0.445(Pr)^{2/3})^{-2/5}(Gr_x)^{2/5} \qquad (36)$$

A. Emery and N. C. Chu (2) conducted an analysis of the heat transfer through vertical plane layers by free convection by means of integral equations and compared these with measured data. They showed that a characteristic heat transfer equation could be expressed in the form:

$$Nu = C(\frac{H}{W})^m (GrPr)^n \qquad (37)$$

for laminar flow and for $Pr = 0.72$ (air)

$$C = 0.246 \qquad m = -1/4 \qquad n = 1/4$$

It is apparent that an exact analytic solution to the problem of natural convection heat transfer in a vertical channel is extremely difficult, perhaps impossible. Because of this an experimental study has been undertaken to provide correlation of pertinent dimensionless parameters which may be used for design purposes. This experimental approach is the subject of this thesis.

DISCUSSION OF APPARATUS AND TEST

General

The main body of the experimental equipment used in this work was made in 1968 by Mr. S. M. Lee (4). For some descriptions concerning parts of the main body of the apparatus, especially the inner portion of the isothermal wall assembly, Lee's work should be consulted.

Figures 2 and 3 are shown to assist in subsequent discussions. Figure 2 shows the whole apparatus and Figure 3 is a schematic drawing of the main portion.

Hot Plate Assembly

This consisted of a liquid acetone boiling chamber, gaseous acetone heat reservoir and an isothermal hot aluminum plate. The electric power was controlled by a variable transformer which controlled the rate of boiling acetone by the power supplied to a resistance heater immersed in the liquid. When starting this operation, the generated acetone vapor which is heavier than the air would drive the air out of the opening at the top of the heat reservoir. The opening is connected to a water-aspirator with polyvinyl tube which was resistant to the hot acetone vapor. Under standard atmospheric pressure

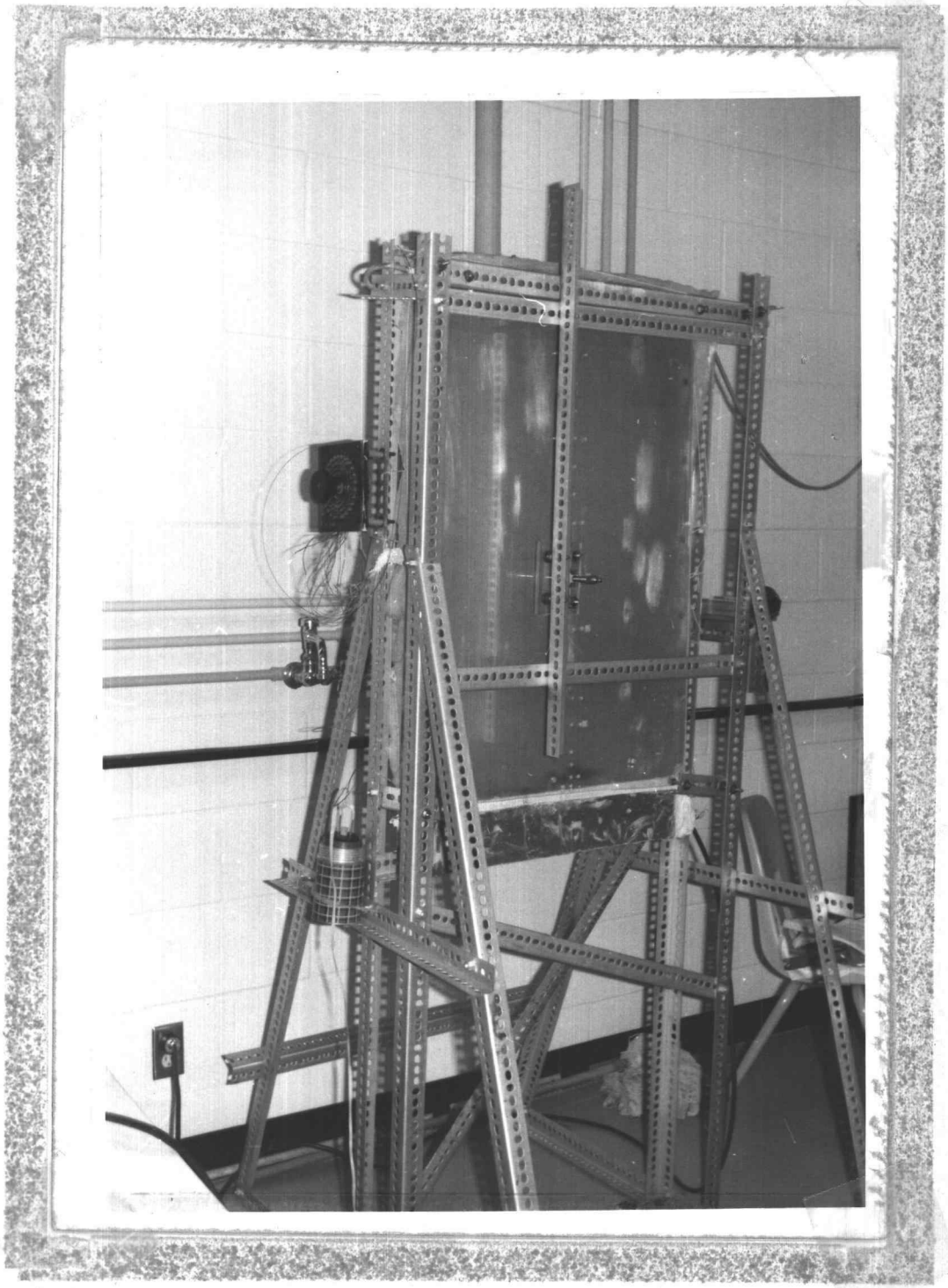

Figure 2. Whole View of Apparatus.

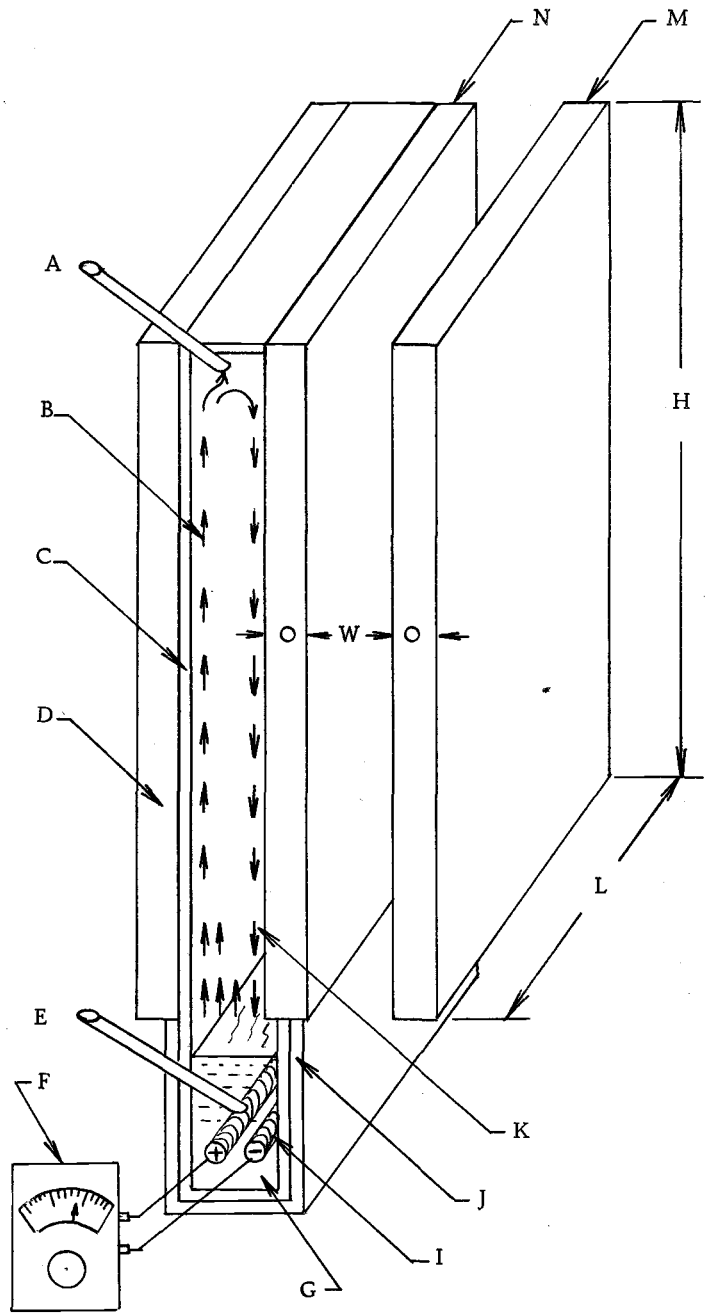

A Leading tube to water-aspirator
B Vapor acetone
C Heat reservoir
D Fiberglass for insulation
E Refilling port
F Transformer
G Liquid acetone
H 38 inches
I Heating element
J Insulating Material
K Condensed acetone
L 24 inches
M Adiabatic wall
N Hot wall
O 3/8 inches
W Air layer spacing

Figure 3. Schematic drawing of two vertical plates.

the boiling point of liquid acetone is 133.2 F. By controlling both the electric power level with the transformer and pressure drop at the end of the connecting tube with the water-aspirator, the pressure inside the heat reservoir could be maintained at a uniform level. Surface temperature was checked with the 15 copper-constantan thermocouples imbedded in the aluminum plate. The dimensions of the plate and the positions of thermocouples are shown in Figure 4. Liquid aluminum was used to fix each thermocouple junction in position and the thermocouple leads were connected to a Millivolt Potentiometer. Usually the outer surface temperature of the aluminum plate was kept between 132 F and 133 F. The temperature distribution along the vertical direction of the plate was made uniform by manipulating both the transformer and water-aspirator. All surfaces except the hot plate were insulated with fiberglass and other insulating materials to decrease heat dissipation through these surfaces as much as possible. Actually heat was transported to the air layer not only by convection but also by radiation which affected the data and will be discussed later. The influence from the radiation heat transfer could be safely neglected by the facts that the temperature difference between hot plate and the ambient was comparatively low and the emissivity of the aluminum plate was very low, its value being 0.07. Before the series of measurements were taken, special care was taken to position the hot plate vertically.

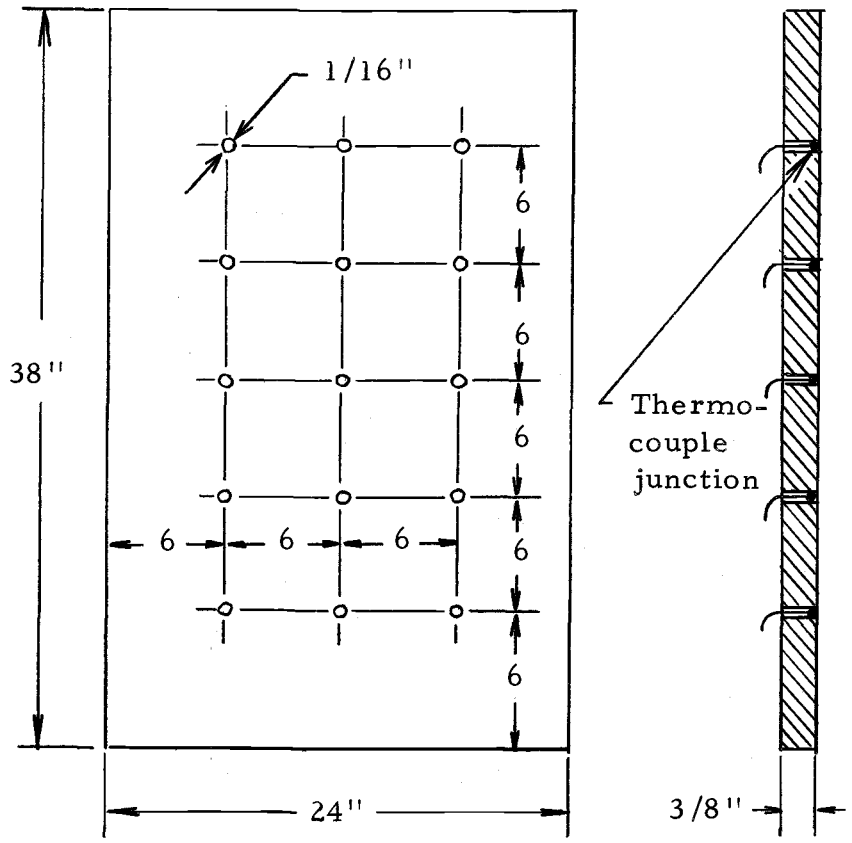

Figure 4. Positions of Thermocouples on Hot Plate.

Adiabatic Plate Assembly

The dimensions of the adiabatic plate were the same as for the aluminum plate: specifically 3/8 in. thick, 24 in. wide and 38 in. high. The reason why plexiglass was chosen as the insulated plate may be explained by its relatively low thermal conductivity and its transparency, which made it possible to measure the deflection of the quartz fiber by viewing through the plexiglass. This plate was supported by two rods protruding from the frame. To align this plate

parallel to the hot plate three sets of spacers (0.625 in., 1.0 in., 1.75 in.) were used. There were five spacers in each set; four were placed in the corners of the plate, and one was near the position of measurement to assure that the distance between the plates was accurate.

Measuring Devices

A thin iron-constantan thermocouple 0.001 in. in diameter was used to measure temperature at a point in the air layer.

To measure the point velocities in the air layer a thin quartz fiber, 0.0005 in. in diameter and 0.45 in. in length was used. Observations were made of the fiber deflection with a cathetometer. Calibration was required to convert the deflection readings into velocities. The procedure and data are illustrated in the following section and in the Appendix.

The quartz fiber and thermocouple were attached to the tip of a thin steel plate (0.025 in. thick, 1/5-1 in. wide, 1 ft. long) mounted on a traversing mechanism which could be located accurately.

Calibration of Quartz Fiber and the Results

Considerable care and precision were taken for accurate calibration of this device. Both the calibration and measurements were accomplished during the night time when the air conditioning system

of the building was shut down to exclude the influence of air currents.

The schematic drawing shown in Figure 5 will be helpful for understanding the calibration procedure of the quartz fiber.

The source of air flow was compressed air provided in the laboratory. Previously a pump was used to supply air, but due to the violent pulsations of the pump, the results were unsatisfactory. The rate of air flow from the building supply system was easily controlled with a needle valve.

For the purpose of measuring the amount of air flow a wet test precision flow meter was used. While the minimum flow rate could be accurately maintained as low as desired, due to the characteristic water sealing mechanism of the measuring chamber, the maximum flow rate was restricted at 1.04 $ft.^3$/min.when the pressure difference between the surroundings and the measuring chamber showed 2 in. of water. This value was taken as the limit for adequate chamber water sealing. Another delicate problem of calibration was the generation of a uniform air velocity distribution across the opening where quartz fiber deflections were measured. Although it was impossible to achieve an absolutely uniform velocity it could be closely approximated by using a smoothly converging nozzle, 1.501 in. in diameter. Deflections corresponding to known air velocities were obtained from the cathetometer readings. Those data are given in Table 1 (Appendix) and are plotted in Figure 6.

A Compressed air

B Air strainer

C Regulator

D Needle valve

E Wet test precision flow meter

F Circular duct

G Bell shape, smoothly converging nozzle of 1.501 in. dia.

H Quartz fiber

I Telescope

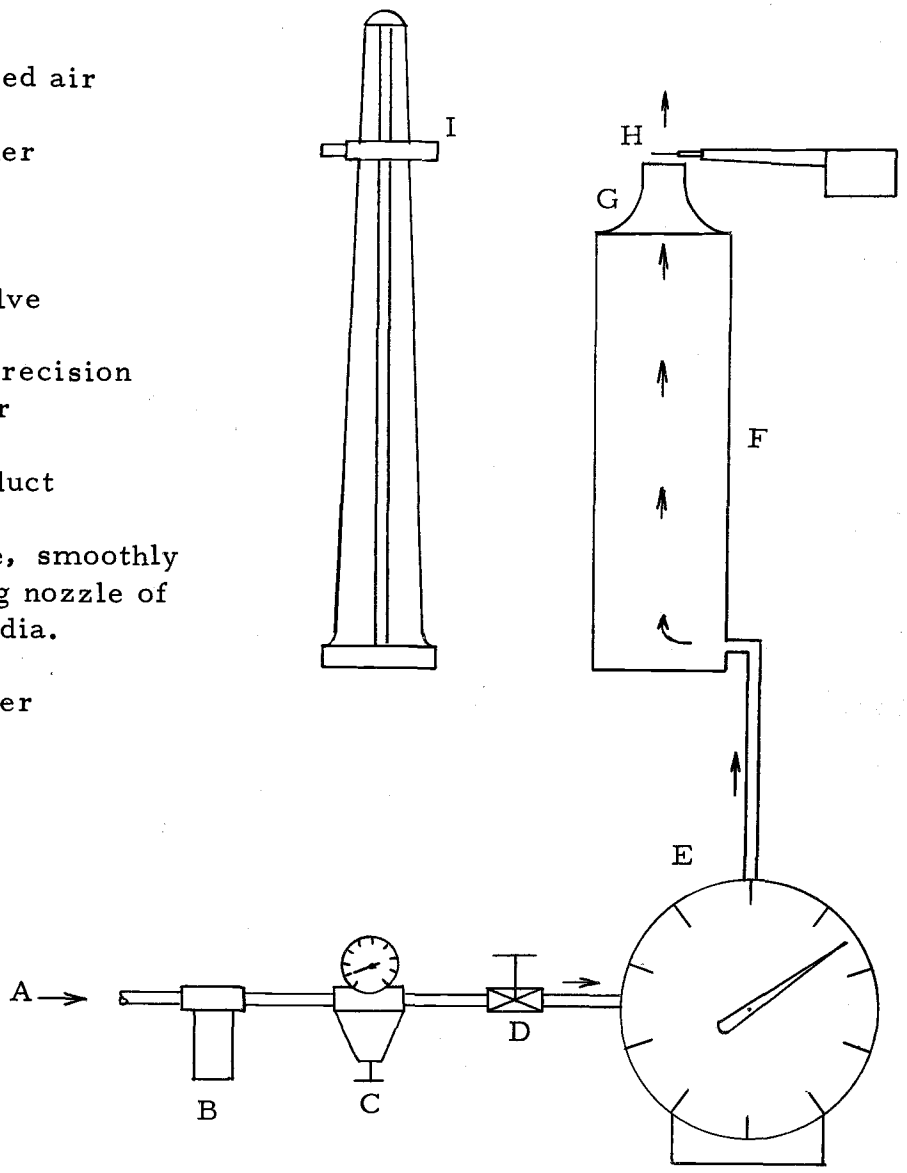

Figure 5. Calibration apparatus of quartz fiber.

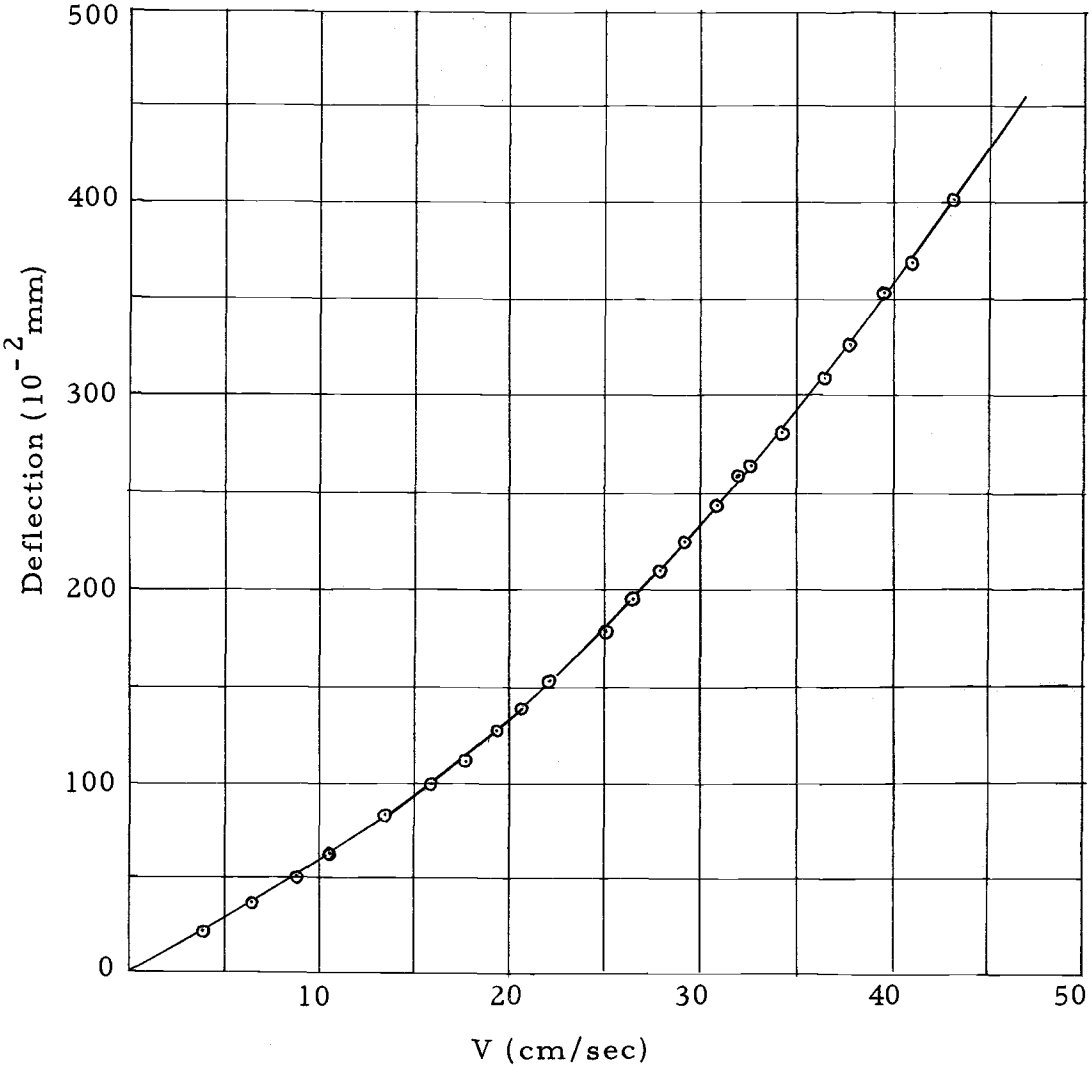

Figure 6. Graph of quartz fiber calibration.

RESULTS

As mentioned in the previous section, low air velocities could be measured easily and accurately with the quartz fiber anemometer. A thermocouple with wire diameter of 0.001 in. was used for measuring air temperatures. During a series of measurements about 0.5 F variation in room temperature occurred, but the accuracy of the results was not affected significantly.

The velocity and temperature distributions across the air layer between the two plates are given in Figures 7, 8, 9 and 10, 11, 12 for spacings of 0.625 in., 1.0 in. and 1.75 in., respectively.

Comparing these data with the isothermal single vertical plate case, it was expected that in the region of $0 < y/W < 0.4$, velocity will increase smoothly to a maximum and then start to decrease; however for the region where $0.4 < y/W < 1.0$, velocities did not always decrease in a regular manner as predicted for the single vertical plate case. A significant variation with vertical position can be seen in the case of velocity profiles in the region of $y/W > 0.4$ particularly those at the smaller x values. The temperature distribution of Figures 10, 11 and 12 indicate the reason for this behavior. The temperature gradient at $y/W = 1.0$ is generally either positive or negative which means heat is either dissipated to the air layer from the insulated plate or conduction occurs from the air layer to the insulated plate.

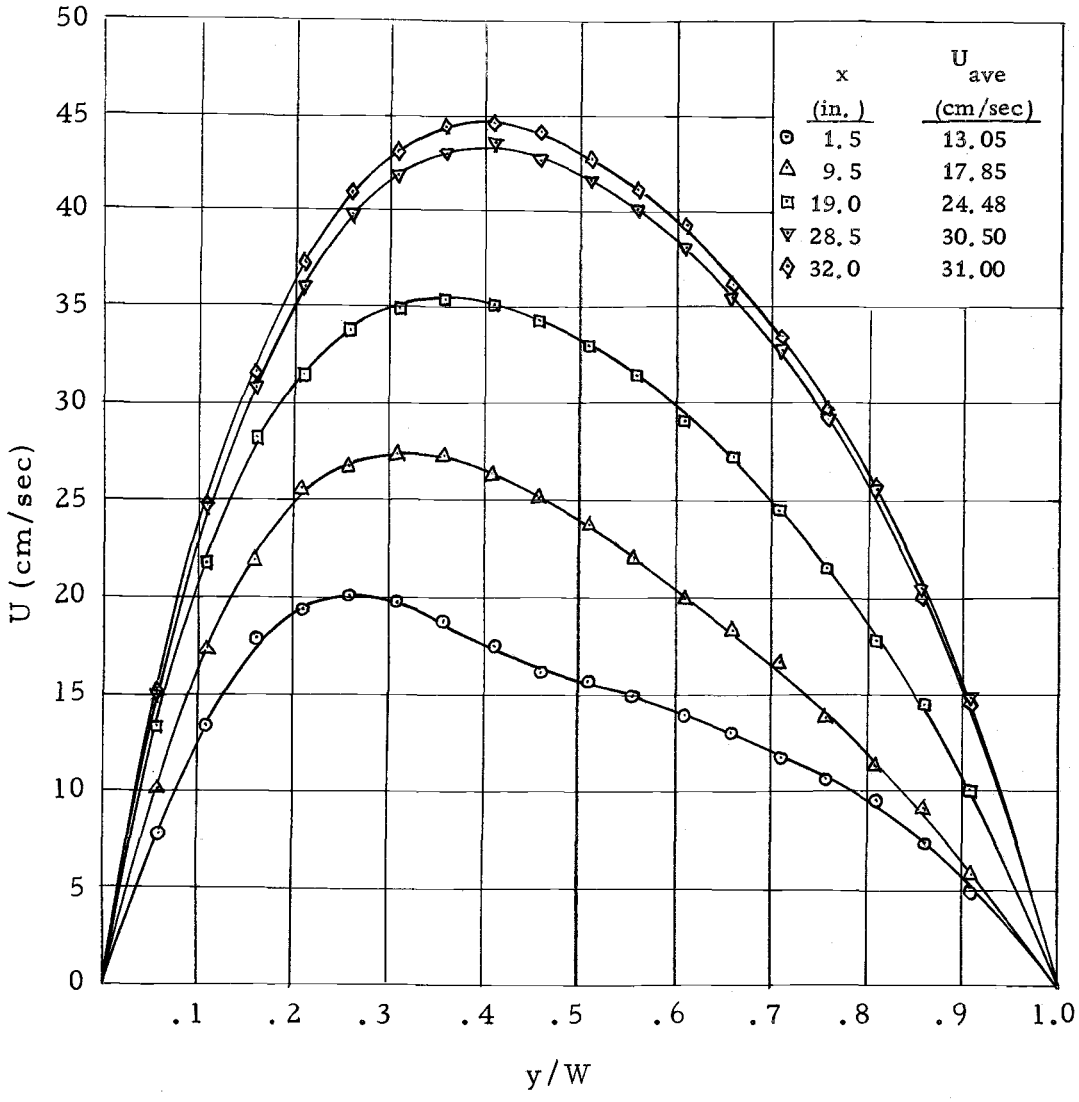

Figure 7. Velocity profiles at several locations; spacing W = 0.625 in.

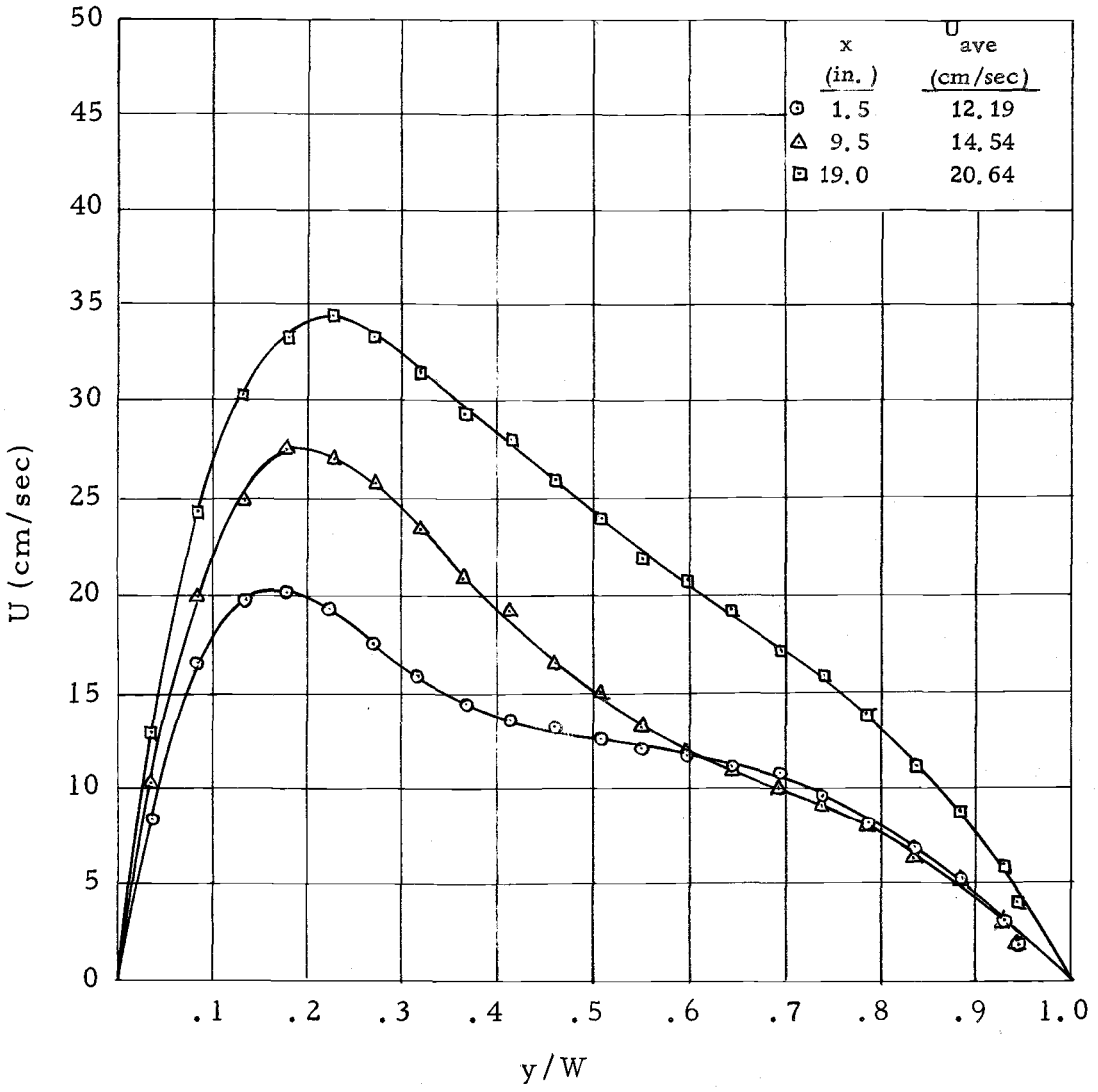

Figure 8. Velocity profiles at several locations; spacing W = 1.0 in.

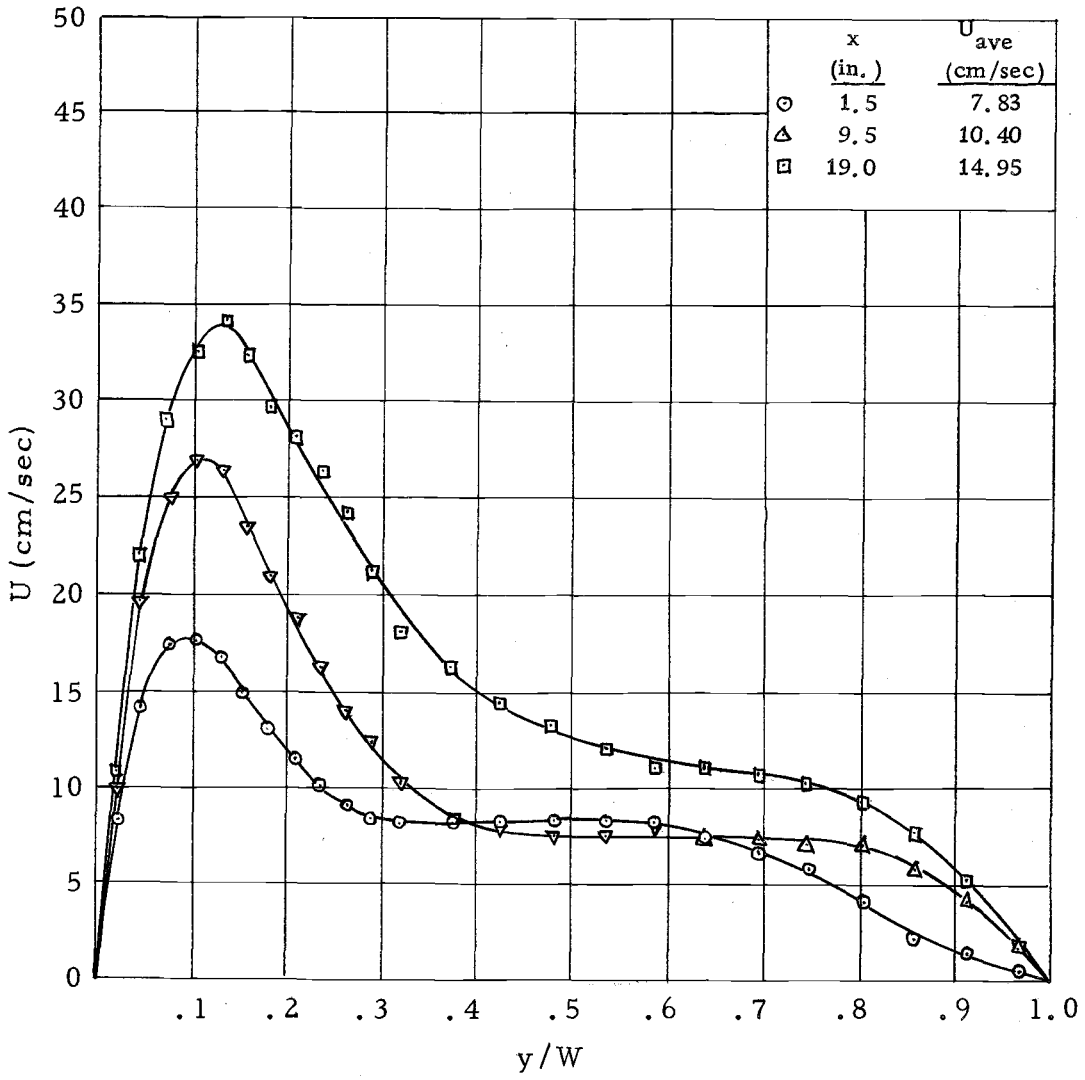

Figure 9. Velocity profiles at several locations; spacing W = 1.75 in.

In practice, an absolutely insulated wall condition can not exist, since heat will be transported to the insulated plate by both radiation and conduction, but no material possesses absolutely zero absorptivity and thermal conductivity. If heat were dissipated from the insulated plate to the air layer, this plate would act as another hot plate and would produce an additional velocity distribution of smaller magnitude. Several velocity curves in Figures 7, 8 and 9 could be assumed as combinations of these two effects. In general the magnitude of the secondary velocity distribution is not significant and was neglected in the following calculations.

For each curve values of the product, UT, was calculated and plotted across the air space to obtain $\int_0^w UTdy$. To obtain T_m (mean temperature of the air layer), U_{ave} was calculated as,

$$U_{ave} = \frac{1}{W} \int_0^w Udy \tag{38}$$

$$T_m = \frac{1}{U_{ave} W} \int_0^w TUdy \tag{39}$$

From the temperature profiles, the temperature gradient of the air layer at the surface of the hot plate, $\frac{dT}{dy})_{y=0}$, was found.

$$q = -k\frac{dT}{dy})_{y=0} = h(T_s - T_m) \tag{40}$$

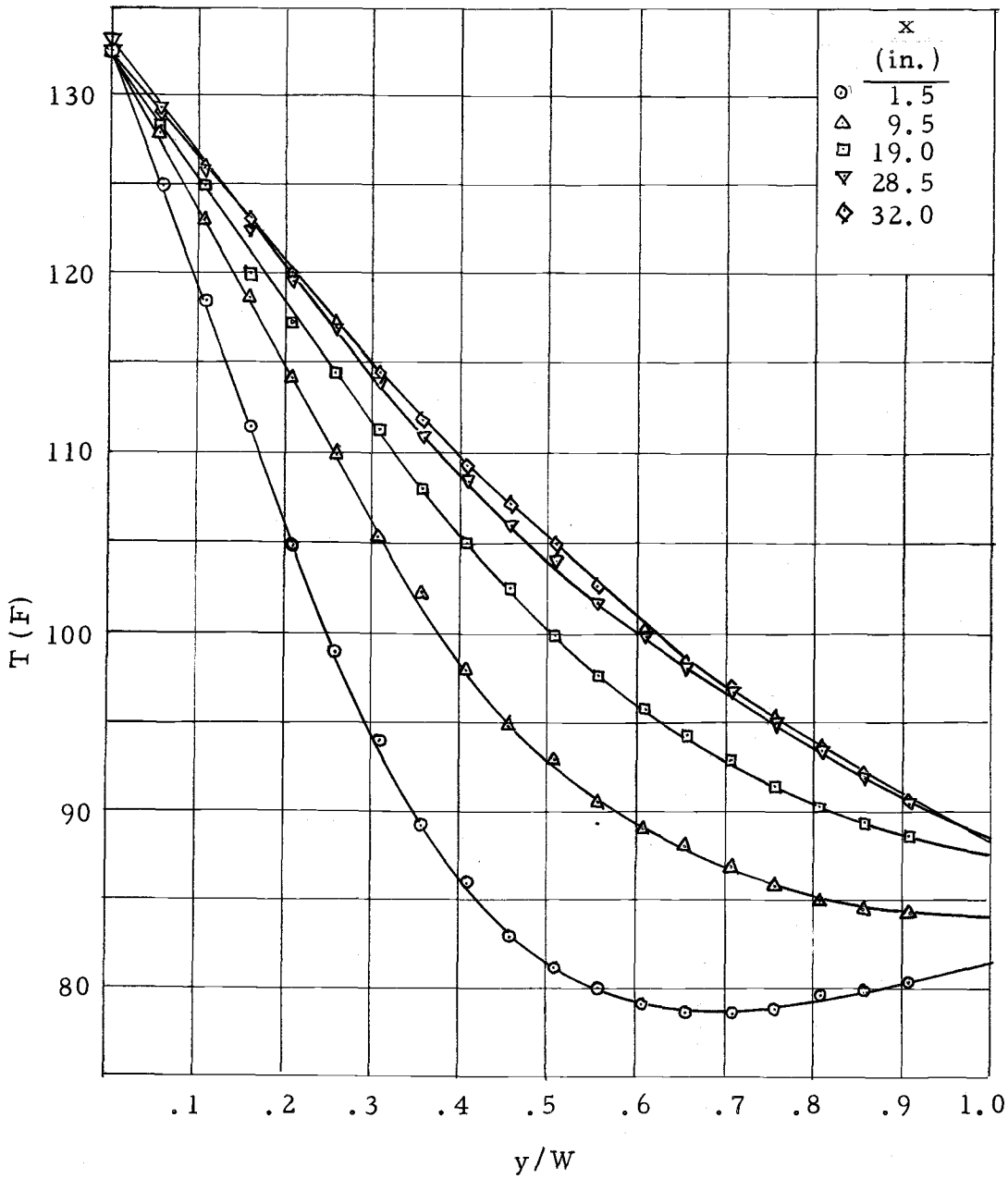

Figure 10. Temperature profiles at several locations; spacing W = 0.625 in.

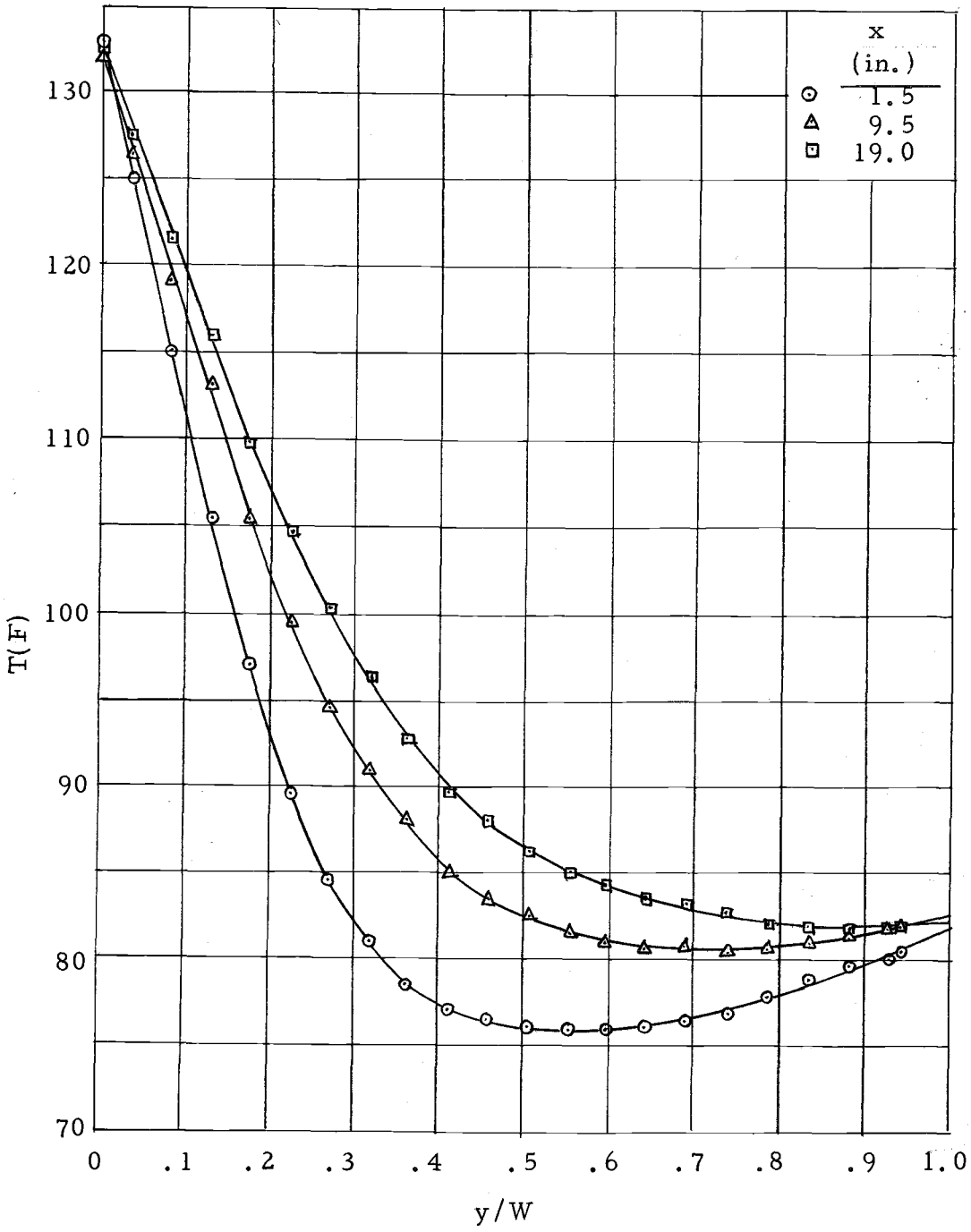

Figure 11. Temperature profiles at several locations; spacing W = 1.0 in.

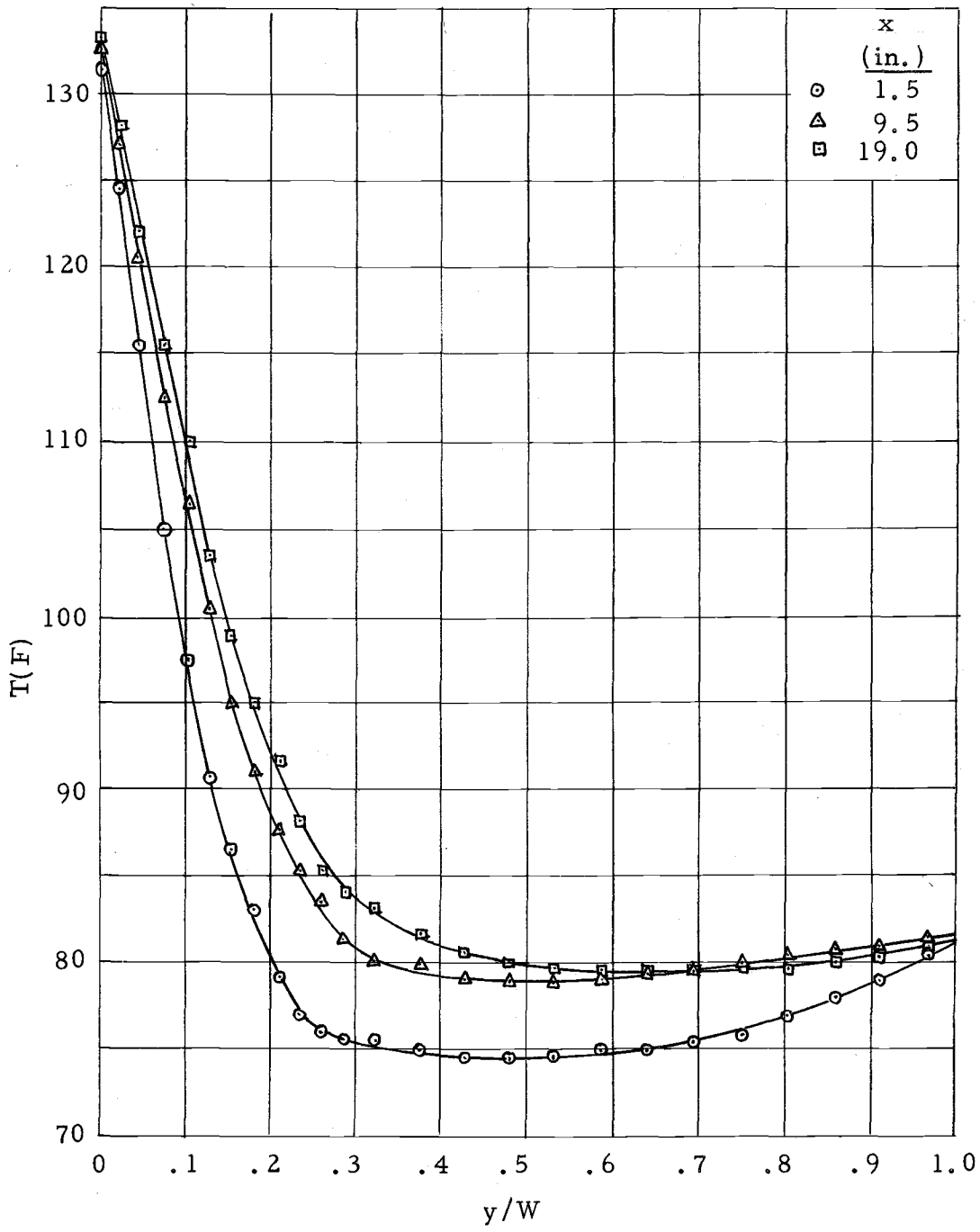

Figure 12. Temperature profiles at several locations; spacing W = 1.75 in.

$$Nu_x = \frac{hx}{k} = -\frac{dT}{dy})_{y=0} \frac{x}{(T_s - T_m)} \tag{41}$$

Various models were used to correlate the local Nusselt number with several dimensionless parameters such as Gr_x, Gr_W, W/H, x/H and x/W, where the physical properties for air were evaluated at the mean temperature of the air layer. The relations between local Nusselt number and $Gr_W(x/H)$, $Gr_x(W/H)$ and $Gr_x(x/W)$ were given particular attention. The numerical values are given in the Appendix and the graphical results are shown in Figures 13, 14 and 15. From these three graphs, the local Nusselt number is related to $Gr_x(x/W)$ in a single equation as

$$Nu_x = 0.348 \, (Gr_x(x/W))^{0.241} \tag{42}$$

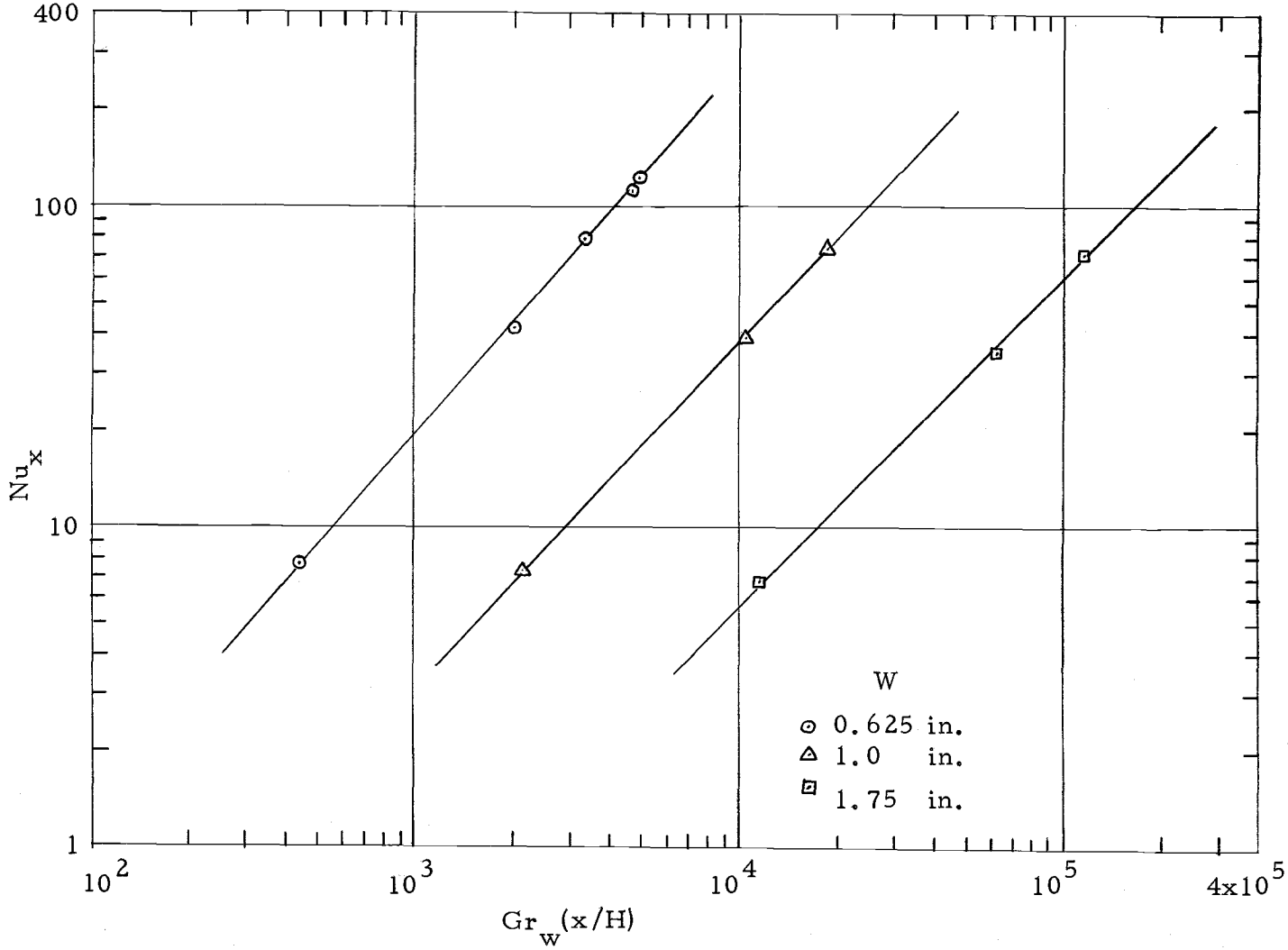

Figure 13. Correlation between local Nusselt number and $Gr_w(x/H)$

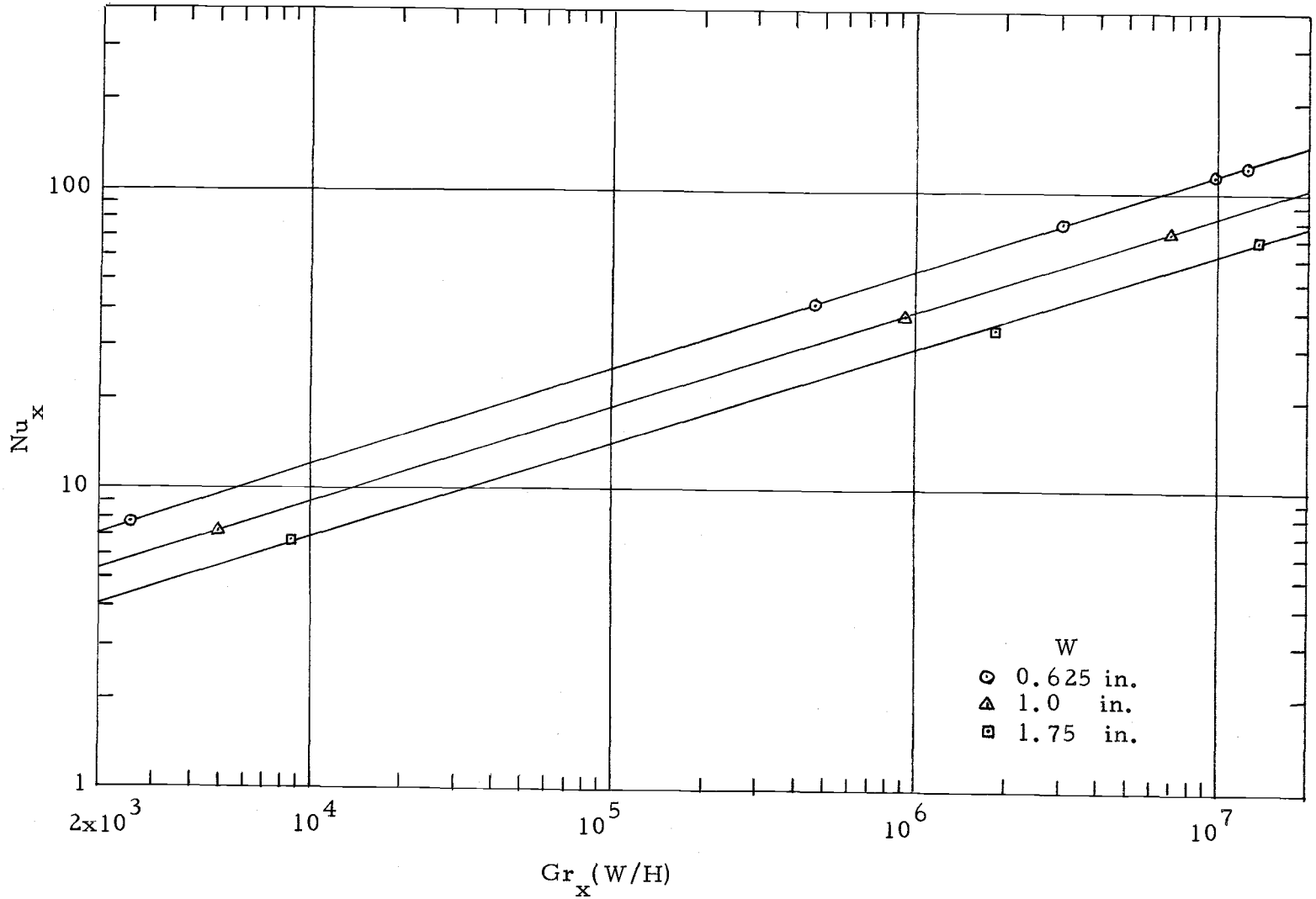

Figure 14. Correlation between local Nusselt number and $Gr_x(W/H)$

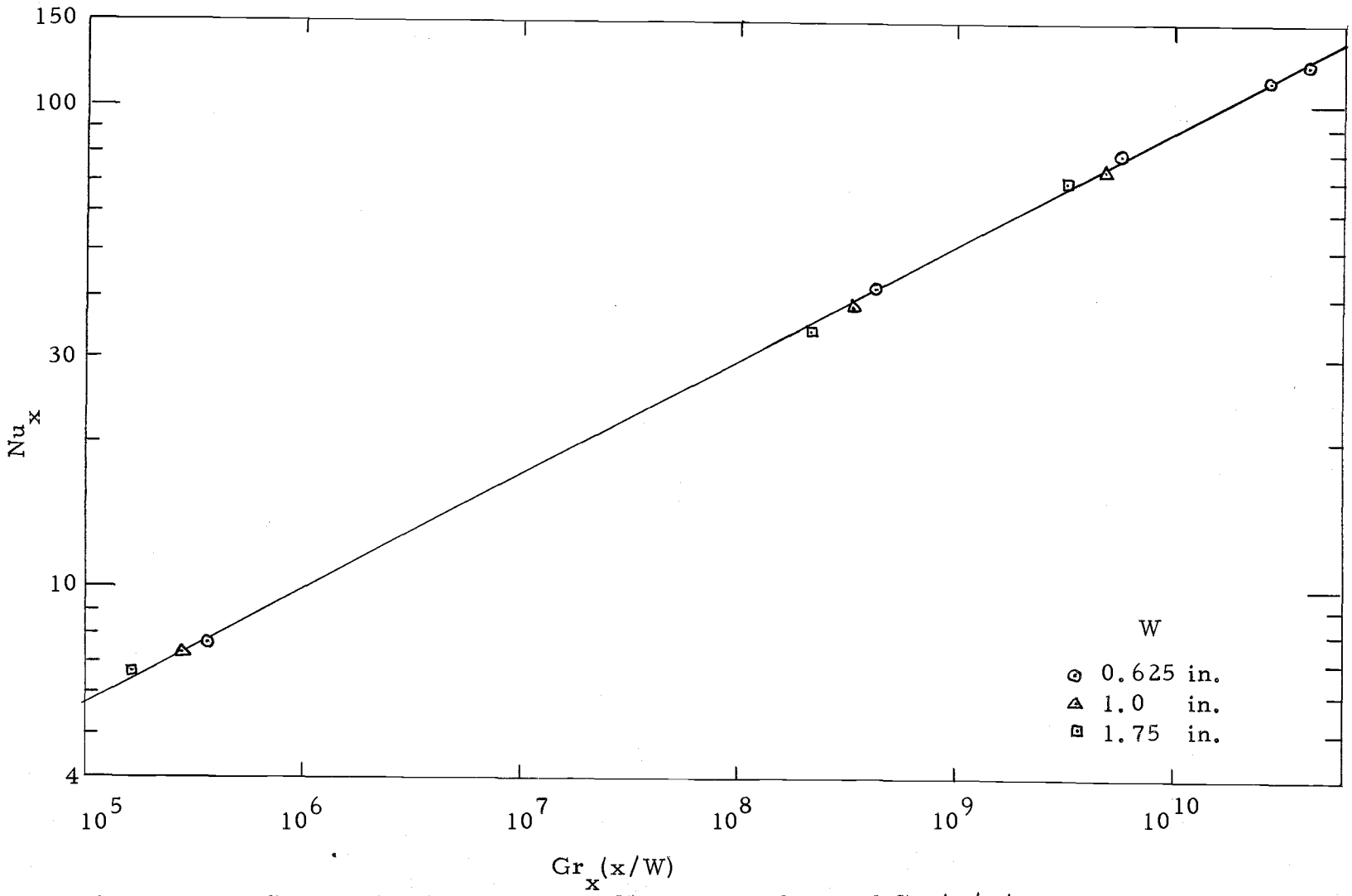

Figure 15. Correlation between local Nusselt number and $Gr_x(x/W)$

CONCLUSION

The performance of the velocity and temperature measuring devices used in this work proved to be very satisfactory. The hand-made quartz fiber velocity measuring device maintained good stability throughout the experiment. No difficulty was encountered with the thermocouple used in determining temperature profiles.

With these devices the data for velocity and temperature distributions in the air space between two vertical plates were obtained. The relationship between local Nusselt number and other dimensionless parameters was found by correlating the experimental data. As a result, the local convective heat transfer coefficient was predicted for the particular situation of a vertical isothermal hot plane surface and a parallel insulated plane surface.

Even though the local Nusselt number turned out not to be a function of the height of the plates according to equation (42), it may be worthwhile to check this result further with different sized plates in both height and width. Additionally, a better adiabatic wall condition should be attempted by using a less conductive material with lower absorptivity without the restriction of transparency which can be overcome by measuring the quartz fiber deflection from the side.

BIBLIOGRAPHY

1. Bevans, J. T. Vertical free convection from an isothermal surface. Industrial and Engineering Chemistry 49:114-119. 1956.

2. Emery, A. and Chu, N. C. Heat transfer across vertical layers. Transactions of the American Society of Mechanical Engineers 84:110-114. 1965.

3. Hsu, S. T. Engineering heat transfer. Chap 11:354-393, Princeton, N. J., Van Nostrand, 1963.

4. Lee, S. M. An experimental study of natural convection in air between a vertical isothermal flat plate and a parallel insulated flat plate. M. S. thesis, Corvallis, Oregon State University, 1969. 85 numb. leaves.

5. Lorenz, L. Ueber das Leitungsvermongen der metalle fuer warme und electricitat. Wiedemanns Annalender Physik und Chemie 13:581-582. 1881.

6. Ostrach, S. An analysis of laminar free-convection flow and heat transfer about a flat plate parallel to the direction of the generating body force. In: Thirty-ninth annual report of the National Committee of Aeronautics, including technical reports. Technical report no. 1111. Washington, D. C., U. S. Government Printing Office, 1955. p. 63-79.

7. Pagnani, B. R. An experimental finite-difference solution for natural convection in air in rectangular enclosures. Ph. D. thesis. Corvallis, Oregon State University, 1968. 176 numb. leaves.

8. Schmidt, E. and Beckmann, W. Das Temperatur und Geschwindingkeitfeld vor einer warme abgebenden senkrechten platte bei naturlecher Konvektion. Technishe Mechanik und Thermodynamik 10:341-349; 11:391-405. 1930.

9. Sparrow, E. M. and J. L. Gregg. Laminar free convection from a vertical plate with uniform surface heat flux. Transactions of the American Society of Mechanical Engineers 78:435-441. 1956.

10. Sparrow, E. M. and J. L. Gregg. The variable fluid-property problem in free convection. Transactions of the American Society of Mechanical Engineers 80:789-886. 1958.

APPENDIX

Table 1. Calibration data for quartz fiber.

Deflection (x 10^{-2} mm)	Velocity (cm. sec.)
20.5	3.9
37.5	6.5
51	8.7
63	10.5
83	13.5
101	15.7
114	17.7
127	19.2
139	20.6
154	22.1
179	25.1
195	26.5
210	27.8
224	29.1
243	30.7
260	32.0
264	32.5
279	34.0
309	36.3
326	37.7
354	39.5
370	40.9
402	43.0

Table 2. Velocity and temperature data.

y(mm)	y/W	$\delta(x10^{-2}$ mm)	U(cm/sec)	T(F)	UT(F-cm/sec)
0.90	0.057	45	7.8	125.0	975
1.695	0.107	83	13.5	118.4	1598
2.489	0.157	118	18.1	111.6	2018
3.284	0.207	131	19.6	104.8	2052
4.078	0.257	137	20.2	99.0	2000
4.873	0.307	132	19.7	94.0	1851
5.667	0.357	126	19.0	89.3	1696
6.462	0.407	114	17.6	86.0	1512
7.256	0.457	107	16.7	83.0	1386
8.051	0.507	101	15.9	81.2	1291
8.845	0.557	94	15.0	80.0	1200
9.640	0.607	87	14.0	79.1	1107
10.435	0.657	81	13.2	78.8	1040
11.229	0.707	72	11.9	78.8	938
12.002	0.757	65	10.9	79.1	862
12.817	0.807	55	9.4	79.7	749
13.611	0.857	42	7.3	80.0	584
14.406	0.907	28	5.0	80.4	402

W = 0.625 in. x = 1.5 in.

Table 2. Continued

y(mm)	y/W	$\delta(x10^{-2}$ mm)	U(cm/sec)	T(F)	UT(F-cm/sec)
0.90	0.057	60	10.15	127.8	1296
1.695	0.107	113	17.4	123.0	2140
2.489	0.157	152	22.0	118.6	2610
3.284	0.207	188	25.7	114.2	2938
4.078	0.257	201	27.0	110.0	2966
4.873	0.307	206	27.4	105.3	2892
5.667	0.357	207	27.5	102.3	2812
6.462	0.407	196	26.5	98.0	2596
7.256	0.457	184	25.35	95.0	2405
8.051	0.507	169	23.9	92.9	2220
8.845	0.557	154	22.2	90.6	2010
9.640	0.607	135	20.1	89.0	1789
10.435	0.657	122	18.6	88.0	1636
11.229	0.707	106	16.6	86.8	1440
12.002	0.757	86	13.9	85.7	1191
12.817	0.807	69	11.5	85.0	977
13.611	0.857	53	9.1	84.5	769
14.406	0.907	33	5.9	84.2	497

W = 0.625 in. x = 9.5 in.

Table 2. Continued

y(mm)	y/W	$\delta(x10^{-2}$ mm)	U(cm/sec)	T(F)	UT(F-cm/cm)
0.90	0.057	82	13.3	128.2	1705
1.695	0.017	152	22.0	124.9	2744
2.489	0.157	214	28.2	120.0	3385
3.284	0.207	254	31.7	117.3	3720
4.078	0.257	282	34.1	114.2	3900
4.873	0.307	293	35.0	111.4	3900
5.667	0.367	299	35.5	108.0	3835
6.462	0.407	296	35.2	105.0	3698
7.256	0.457	286	34.4	102.5	3525
8.051	0.507	268	32.9	100.0	3290
8.845	0.557	251	31.5	97.7	3080
9.640	0.607	225	29.2	96.0	2800
10.435	0.657	203	27.2	94.3	2564
11.229	0.707	176	24.6	92.8	2282
12.002	0.757	148	21.6	91.5	1976
12.817	0.807	116	17.8	90.2	1605
13.611	0.857	90	14.5	89.4	1295
14.406	0.907	60	10.1	88.6	895

W = 0.625 in. x = 19 in.

Table 2. Continued

y(mm)	y/W	$\delta(x10^{-2}mm)$	U(cm/sec)	T(F)	UT(F-cm/sec)
0.90	0.057	96	15.2	129.2	1797
1.695	0.107	180	24.9	126.0	3140
2.489	0.157	244	30.8	122.4	3770
3.284	0.207	308	36.2	119.6	4330
4.078	0.257	354	39.7	116.9	4640
4.873	0.307	386	42.0	113.9	4780
5.667	0.357	400	43.0	111.0	4780
6.462	0.407	405	43.4	108.4	4700
7.256	0.457	397	42.8	106.0	4540
8.051	0.507	381	41.7	104.0	4340
8.845	0.557	361	40.2	101.8	4090
9.640	0.607	333	38.1	100.0	3810
10.435	0.657	300	35.5	98.2	3530
11.229	0.707	266	32.7	96.7	3160
12.002	0.757	224	29.2	95.0	2772
12.817	0.807	186	25.5	93.6	2385
13.611	0.857	136	20.3	92.0	1868
14.406	0.907	91	14.7	90.6	1332

W = 0.625 in. x = 28.5 in.

Table 2. Continued

y(mm)	y/W	$\delta(x10^{-2}mm)$	U(cm/sec)	T(F)	UT(F-cm/sec)
0.90	0.057	97	15.4	129.0	1985
1.695	0.107	177	24.7	126.0	3115
2.489	0.157	256	31.7	123.0	3900
3.284	0.207	320	37.2	120.0	4460
4.078	0.257	372	41.0	117.2	4810
4.873	0.307	403	43.2	114.5	4950
5.667	0.357	419	44.4	112.0	4975
6.462	0.407	421	44.6	109.2	4875
7.256	0.457	413	44.0	107.2	4720
8.051	0.507	397	42.8	105.0	4500
8.845	0.557	376	41.3	102.7	4240
9.640	0.607	347	39.2	100.2	3930
10.435	0.657	307	36.1	98.0	3540
11.229	0.707	271	33.1	97.1	3210
12.002	0.757	228	29.4	95.2	2804
12.817	0.807	182	25.2	93.6	2355
13.611	0.857	132	19.8	92.0	1821
14.406	0.907	88	14.2	90.2	1281

W = 0.625 in. x = 32 in.

Table 2. Continued

y(mm)	y/W	$\delta(\times 10^{-2}$ mm)	U(cm/sec)	T(F)	UT(F-cm/sec)
0.90	0.035	50	8.6	125.0	1075
2.092	0.082	108	16.8	115.0	1930
3.284	0.129	132	19.8	105.5	2090
4.475	0.176	136	20.2	97.0	1960
5.667	0.223	128	19.2	89.5	1710
6.859	0.270	116	17.6	84.5	1490
8.051	0.317	101	15.9	81.0	1290
9.243	0.364	91	14.6	78.5	1145
10.434	0.411	84	13.6	77.0	1047
11.626	0.458	81	13.2	76.5	1010
12.818	0.505	78	12.8	76.2	976
14.010	0.552	74	12.2	76.0	927
15.202	0.599	71	11.7	76.0	890
16.394	0.646	68	11.3	76.2	861
17.585	0.693	64	10.7	76.5	819
18.777	0.740	57	9.7	77.0	747
19.969	0.787	46	8.0	77.8	622
21.161	0.834	39	6.9	78.5	541
22.352	0.881	29	5.2	79.5	413
23.544	0.928	16	3.0	80.0	240
23.901	0.941	9	1.7	80.5	137

W = 1.0 in. x = 1.5 in.

Table 2. Continued

y(mm)	y/W	$\delta(x10^{-2}mm)$	U(cm/sec)	T(F)	UT(F-cm/sec)
0.90	0.035	61	10.3	126.5	1300
2.092	0.082	134	20.0	119.0	2380
3.284	0.129	182	25.0	113.0	2825
4.475	0.176	204	27.6	105.5	2910
5.667	0.223	201	27.0	99.5	2685
6.859	0.270	187	25.7	94.5	2430
8.051	0.317	163	23.3	91.0	2120
9.243	0.364	143	21.0	88.0	1850
10.434	0.411	124	19.3	85.0	1640
11.626	0.458	107	16.7	83.5	1394
12.818	0.505	95	15.1	82.5	1245
14.010	0.552	83	13.5	81.5	1100
15.202	0.599	71	11.8	81.0	955
16.394	0.646	63	10.6	80.7	855
17.585	0.693	58	9.8	80.7	791
18.777	0.740	52	8.9	80.5	716
19.969	0.787	45	7.9	80.6	637
21.161	0.834	37	6.5	81.0	526
22.352	0.881	29	5.3	81.5	432
23.544	0.928	16	3.0	81.7	245
23.901	0.941	12	2.2	82.0	180

W = 1.0 in. x = 9.5 in.

Table 2. Continued

y(mm)	y/W	$\delta(x10^{-2}mm)$	U(cm/sec)	T(F)	UT(F-cm/sec)
0.90	0.035	78	13.0	127.5	1655
2.092	0.082	173	24.3	121.5	2950
3.284	0.129	238	30.3	116.0	3520
4.475	0.176	277	33.5	109.8	3680
5.667	0.223	285	34.3	104.7	3590
6.859	0.270	276	33.6	100.3	3370
8.051	0.317	257	31.8	96.3	3060
9.243	0.364	234	29.5	92.7	2738
10.434	0.411	210	28.0	89.7	3510
11.626	0.458	191	26.0	87.8	2282
12.818	0.505	172	24.1	86.2	2080
14.010	0.552	153	22.1	85.0	1880
15.202	0.599	142	20.9	84.2	1760
16.394	0.646	124	18.8	83.6	1570
17.585	0.693	111	17.2	83.0	1430
18.777	0.740	99	15.7	82.7	1300
19.969	0.787	85	13.8	82.1	1132
21.161	0.834	67	11.2	82.0	919
22.352	0.881	51	8.8	81.8	720
23.544	0.928	33	5.9	81.7	482
23.901	0.941	22	4.0	81.6	326

W = 1.0 in. x = 19 in.

Table 2. Continued

y(mm)	y/W	$\delta(x10^{-2}mm)$	U(cm/sec)	T(F)	UT(F-cm/sec)
0.90	0.022	47	8.2	124.5	1020
2.092	0.047	88	14.2	115.5	1640
3.284	0.074	112	17.4	105.0	1825
4.475	0.101	114	17.6	97.5	1715
5.667	0.128	107	16.7	90.5	1500
6.859	0.154	94	15.0	86.5	1300
8.051	0.181	81	13.2	83.0	1075
9.243	0.208	69	11.5	79.0	909
10.434	0.235	60	10.2	77.0	785
11.626	0.262	54	9.2	76.0	700
12.818	0.289	59	8.6	75.5	650
14.202	0.320	48	8.4	75.5	635
16.585	0.373	48	8.4	75.0	630
18.969	0.426	47	8.3	74.5	619
21.352	9.480	47	8.3	74.5	619
23.736	0.534	49	8.4	74.8	629
26.120	0.587	47	8.3	75.0	622
28.503	0.641	43	7.5	75.0	563
30.887	0.695	39	6.9	75.5	521
33.270	0.749	32	5.7	76.0	434
35.654	0.802	22	4.1	77.0	316
38.037	0.856	12	2.2	78.0	172
40.421	0.909	8	1.5	79.0	118
42.960	0.966	3	0.5	80.5	42

W = 1.75 in. x = 1.5 in.

Table 2. Continued

y(mm)	y/W	$\delta(x10^{-2}mm)$	U(cm/sec)	T(F)	UT(F-cm/sec)
0.90	0.022	59	10.0	127.0	1270
2.092	0.047	130	19.5	120.4	2350
3.284	0.074	180	25.0	112.5	2810
4.475	0.101	201	27.0	106.5	2875
5.667	0.128	195	26.4	100.5	2655
6.859	0.154	166	23.5	95.0	2230
8.051	0.181	141	20.8	91.0	1890
9.243	0.208	125	18.8	87.5	1645
10.434	0.235	104	16.3	85.2	1405
11.626	0.262	87	14.0	83.5	1170
12.818	0.289	76	12.5	81.4	1050
14.202	0.320	61	10.3	80.1	834
16.585	0.373	49	8.5	79.9	679
18.969	0.426	46	8.0	79.0	632
21.352	0.480	43	7.5	78.9	592
23.736	0.534	44	7.6	78.9	600
26.120	0.587	46	8.0	79.0	632
28.503	0.641	43	7.5	79.3	595
30.887	0.695	43	7.5	79.7	598
33.270	0.749	42	7.3	80.0	584
35.654	0.802	41	7.2	80.3	578
38.037	0.856	33	5.9	80.8	476
40.421	0.909	23	4.3	81.0	351
42.960	0.966	10	1.9	81.6	155

W = 1.75 in. x = 9.5 in.

Table 2. Continued

y(mm)	y/W	$\delta(x10^{-2}mm)$	U(cm/sec)	T(F)	UT(F-cm/sec)
0.90	0.022	65	10.9	128.0	1394
2.092	0.047	154	22.2	122.0	2710
3.284	0.074	222	28.9	115.5	3340
4.475	0.101	265	32.6	110.0	3590
5.667	0.128	283	34.1	103.5	3650
6.859	0.154	262	32.4	99.0	3205
8.051	0.181	240	29.6	95.0	2810
9.243	0.208	214	28.2	91.7	2582
10.434	0.235	193	26.2	88.0	2300
11.626	0.262	172	24.2	85.2	2060
12.818	0.289	143	21.1	84.0	1770
14.202	0.320	118	18.1	83.2	1508
16.585	0.373	105	16.5	81.7	1342
18.969	0.426	91	14.7	80.7	1181
21.352	0.480	82	13.2	80.0	1056
23.736	0.534	74	12.2	79.7	971
26.120	0.587	66	11.0	79.6	876
28.503	0.641	67	11.2	79.6	891
30.887	0.695	64	10.8	79.6	860
33.270	0.749	60	10.2	79.6	812
35.654	0.802	54	9.2	79.7	733
38.037	0.856	45	7.8	80.0	624
40.421	0.909	29	5.2	80.4	418
42.960	0.966	12	2.2	81.0	178

W = 1.75 in. x = 19 in.

Table 3. Nu_x at various points.

W(in)	x(in)	$\frac{dT}{dy})_{y=0}$(F/cm)	T_s(F)	T_m(F)	$T_s - T_m$(F)	Nu_x
0.625	1.5	-84.8	132.8	90.6	42.2	7.65
"	9.5	-57.1	132.8	100.1	32.7	42.1
"	19.0	-45.0	132.5	104.9	27.6	78.9
"	28.5	-40.8	132.9	106.7	26.2	112.7
"	32.0	-38.8	132.8	107.2	25.6	122.3
1.0	1.5	-92.0	132.9	84.5	48.4	7.25
"	9.5	-61.3	132.0	93.4	38.6	38.3
"	19.0	-54.2	132.7	96.9	35.8	73.2
1.75	1.5	-84.4	131.6	83.6	48.0	6.7
"	9.5	-60.6	132.4	89.7	42.7	34.3
"	19.0	-57.0	132.9	93.1	39.8	69.1

Table 4. Correlation between Nu_x and other parameters

W(in)	x(in)	Nu_x	$Gr_w(x/H)$	$Gr_x(W/H)$	$Gr_x(x/W)$
0.625	1.5	7.65	4.46×10^2	2.58×10^3	3.76×10^5
"	9.5	42.1	2.02×10^3	4.67×10^5	4.32×10^8
"	19.0	78.9	3.30×10^3	3.06×10^6	5.65×10^9
"	28.5	112.7	4.65×10^3	9.70×10^6	2.69×10^{10}
"	32.0	122.3	4.90×10^3	1.25×10^7	4.15×10^{10}
1.0	1.5	7.25	2.21×10^3	4.97×10^3	2.82×10^5
"	9.5	38.3	1.04×10^4	9.43×10^5	3.40×10^8
"	19.0	73.2	1.873×10^4	6.98×10^6	4.88×10^9
1.75	1.5	6.7	1.165×10^4	8.66×10^3	1.61×10^5
"	9.5	34.3	6.33×10^4	1.865×10^6	2.20×10^8
"	19.0	69.1	1.16×10^5	1.365×10^7	3.22×10^9